outcome. The extent of NCP was defined as a dichotomous variable for high (≥2) and low (≤1) NCP counts. Stratified analyses were also performed according to the vulnerable NCP characteristics (PR, low CT density, and spotty calcium). Multivariate logistic regression analyses were performed to determine whether the association between VAT area and the presence and extent of NCP was independent of age, sex, and traditional risk factors (hypertension, hypercholesterolemia, diabetes mellitus, and current smoking). We further assessed the relationship between VAT area and the presence of vulnerable NCP characteristics using age- and sex-adjusted, and multivariate logistic regression models in a hierarchal fashion. All analyses were done using JMP 5.0.1 statistical software (SAS Institute Inc., Cary, North Carolina). A p value of <0.05 was considered statistically significant.

RESULTS

Patient characteristics. Table 1 lists the clinical characteristics of the study patients according to the median VAT area (men, 126 cm^2; women, 91 cm^2). Compared with patients with low VAT area, those with high VAT area had a higher BMI, waist circumference, and subcutaneous adipose tissue area, and a higher prevalence of hypertension, hypercholesterolemia, and diabetes mellitus, in both sexes. In addition, the triglyceride and hemoglobin A_{1c} levels were higher and the high-density lipoprotein cholesterol level was lower in patients with high VAT, in both sexes. With respect to medications, patients with high VAT area had a higher prevalence of using antihypertensive agents in men, and hypoglycemic agents in both sexes.

CTA plaque characteristics. Of 427 patients, 95 (22%) had no coronary plaques. Of the remaining 332 (78%) patients, calcified plaques alone were observed in 72 (17%) patients, and NCPs were detected in 260 (61%, 189 men) patients. A total of 576 NCPs were visualized (mean 2.2 ± 1.1 per patient), and the NCPs were localized to the left main trunk (n = 57), left anterior descending artery (n = 245), left circumflex artery (n = 103), and the right coronary artery (n = 171). Of the 427 patients, 120 (28%) had a ≥50% stenotic lesion in at least 1 coronary vessel. The number of patients with NCPs with PR (remodeling index >1.05), low CT density (≤38 HU), and adjacent spotty calcium deposits was 166 (39%), 159 (37%), and 114 (27%), respectively. Seventy-one patients (17%) had NCP with all 3 characteristics.

Table 1. Characteristics of the Study Patients With High and Low VAT Area

	Men (n = 267)		Women (n = 160)	
	High VAT (n = 133)	Low VAT (n = 134)	High VAT (n = 80)	Low VAT (n = 80)
Age, yrs	65 ± 10	64 ± 12	71 ± 10	68 ± 11
BMI, kg/m^2	25.7 ± 2.7†	22.4 ± 3.1	24.7 ± 3.4†	22.1 ± 3.4
WC, cm	95.8 ± 7.5†	84.7 ± 7.6	93.7 ± 7.7†	82.3 ± 8.4
SAT, cm^2	143 ± 53†	99 ± 46	190 ± 71†	141 ± 61
Hypertension, n (%)	92 (69)*	76 (57)	48 (60)*	35 (44)
Hypercholesterolemia, n (%)	80 (60)*	61 (46)	48 (60)*	32 (40)
Diabetes mellitus, n (%)	79 (59)†	50 (37)	41 (51)†	23 (29)
Current smoking, n (%)	73 (55)	66 (49)	13 (16)	6 (8)
Total cholesterol, mg/dl	201 ± 34	196 ± 41	203 ± 39	204 ± 51
Triglycerides, mg/dl	156 (109–231)†	111 (83–157)	146 (110–210)†	98 (75–133)
HDL cholesterol, mg/dl	48 ± 14†	59 ± 18	57 ± 16†	68 ± 17
LDL cholesterol, mg/dl	119 ± 29	114 ± 32	119 ± 35	119 ± 47
HbA_{1c}, %	6.3 ± 1.3†	5.8 ± 1.3	6.3 ± 1.2†	5.8 ± 1.2
Medications				
Antihypertensive agents, n (%)	49 (37)*	32 (24)	20 (25)	22 (28)
Lipid-lowering agents, n (%)	39 (29)	32 (24)	22 (28)	18 (23)
Hypoglycemic agents, n (%)	43 (32)*	27 (20)	28 (35)*	15 (19)

Values are expressed as number (percent), mean ± SD, or medians (interquartile range). High VAT indicates VAT area greater than the sex-specific median value (men, 126 cm^2; women, 91 cm^2), and low VAT indicates VAT area less than the median value. *$p < 0.05$; †$p < 0.01$ versus low VAT group.
BMI = body mass index; HbA1c = hemoglobin A1c; HDL = high-density lipoprotein; LDL = low-density lipoprotein; SAT = subcutaneous adipose tissue; VAT = visceral adipose tissue; WC = waist circumference.

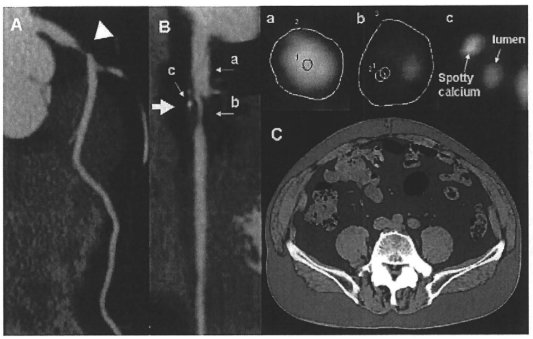

Figure 1. **Coronary CT Angiography in a 74-Year-Old Man With High VAT Presenting With Unstable Angina Pectoris**

(A) Shows a significant stenotic lesion in the proximal left anterior descending artery **(arrowhead)**. The stretched multiplanar reconstruction image of the vessel shows obstructive NCP with positive remodeling and adjacent spotty calcium **(B, arrow)**. The cross-sectional vessel areas of the reference site **(a)** and the lesion **(b)** are 26 and 32 mm^2, respectively. Therefore, the remodeling index is 1.23. The minimum computed tomography (CT) density of the lesion is 21 HU **(b)**. The **small circles** within the outer vessel boundaries indicate regions of interest (area = 1 mm^2) **(a, b)**. Adjacent spotty calcium can be observed in the cross-sectional image **(c)**. **(C)** Shows the abdominal adipose tissue areas at the level of the umbilicus. Regions of **blue** and **red** color indicate visceral (162 cm^2) and subcutaneous (151 cm^2) adipose tissue, respectively. CT = computed tomography; NCP = noncalcified coronary plaque; VAT = visceral adipose tissue.

Comparisons of plaque burden and vulnerable characteristics between patients with high and low VAT area. Figure 1 shows a representative CTA finding in a patient with high VAT area presenting with unstable angina pectoris. Figure 2 shows the prevalence of plaque characteristics in patients with high and low VAT area. Compared with patients with low VAT, men (71% vs. 56%, $p = 0.01$) and women (61% vs. 36%, $p = 0.002$) with high VAT were more likely to have calcified plaque. Similarly, men (82% vs. 60%, $p < 0.0001$) and women (56% vs. 33%, $p = 0.003$) with high VAT were more likely to have NCP. In analyses stratified for vulnerable NCP characteristics, patients with high

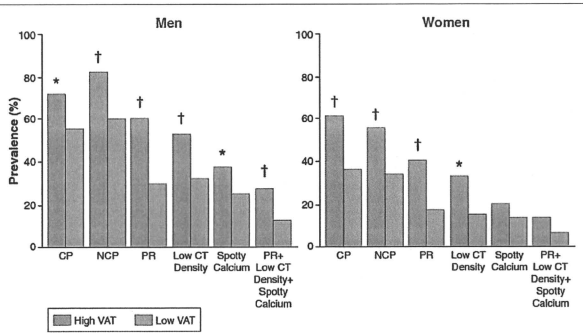

Figure 2. **Prevalence of Plaque Characteristics in Patients With High and Low VAT**

High VAT **(pink bars)** indicates VAT area greater than the sex-specific median value (men 126 cm^2, women 91 cm^2) and low VAT **(green bars)** indicates VAT area less than the median. CP = calcified coronary plaque; PR = positive remodeling; other abbreviations as in Figure 1. *$p < 0.05$; †$p < 0.01$.

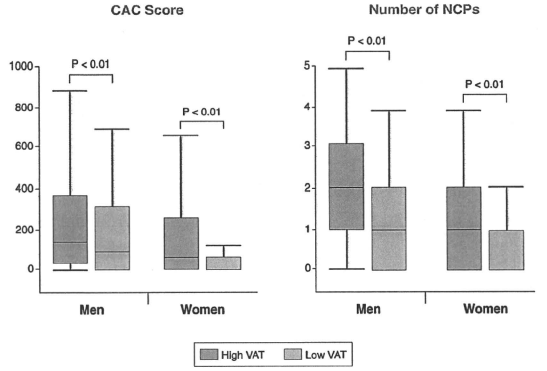

Figure 3. CAC Score and the Number of NCPs in Patients With High versus Low VAT Area

The patients with higher VAT had significantly higher median levels of CAC scores and the number of NCPs in both sexes. **Boxes** indicate 25th and 75th percentiles; **lines** indicate 5th and 95th percentiles for the data. CAC = coronary artery calcium; other abbreviations as in Figure 1.

VAT had a higher prevalence of NCP with PR (59% vs. 30%, $p < 0.0001$), low CT density (55% vs. 34%, $p = 0.0007$), and adjacent spotty calcium (41% vs. 26%, $p = 0.01$) in men, and PR (41% vs. 18%, $p = 0.001$) and low CT density (34% vs. 16%, $p = 0.01$) in women. The frequency of patients with NCP with all 3 characteristics was higher in men with high VAT (29% vs. 13%, $p = 0.001$). Figure 3 shows the CAC score and the number of NCPs for patients with high and low VAT. In both sexes, patients with high VAT area were more likely to have high CAC scores (138 [18 to 342] vs. 60 [0 to 292], $p = 0.008$ in men, 46 [0 to 246] vs. 0 [0 to 45], $p = 0.0001$ in women) and a greater extent of NCP distribution (2 [1 to 3] vs. 1 [0 to 2], $p = 0.004$ in men, 1 [0 to 2] vs. 0 [0 to 1], $p = 0.003$ in women) than those with low VAT.

Multivariate association of VAT area with calcified plaques. Calcified plaques were observed in 247 (58%, 169 men) patients. Multivariate association of VAT area with the presence of calcified plaque is presented in Table 2. As well as age, hypertension, hypercholesterolemia, and diabetes mellitus, increased VAT area was significantly associated with the presence of calcified plaque.

Multivariate associations of VAT area with NCP burden and vulnerable characteristics. Table 3 shows the association between VAT area and clinical variables with the presence and extent of NCP in all patients. In addition to age, sex, and traditional coronary risk

Table 2. Associations With the Presence of Calcified Plaque

	Univariate		Multivariate	
	OR (95% CI)*	p Value	OR (95% CI)*	p Value
Age, per 11 yrs	1.41 (1.16–1.72)	0.0006	1.60 (1.28–2.03)	<0.0001
Sex, men	1.81 (1.22–2.70)	0.003	1.56 (0.96–2.55)	0.07
VAT, per 58 cm^2	1.71 (1.37–2.15)	<0.0001	1.34 (1.05–1.73)	0.02
Hypertension	2.29 (1.55–3.41)	<0.0001	1.62 (1.05–2.50)	0.03
Hypercholesterolemia	1.73 (1.17–2.55)	0.006	1.58 (1.03–2.42)	0.04
Diabetes mellitus	2.33 (1.57–3.49)	<0.0001	2.04 (1.32–3.16)	0.001
Current smoking	1.71 (1.14–2.58)	0.01	1.44 (0.89–2.34)	0.1

*Odds ratio (95% confidence interval) for the presence of calcified plaque associated with the presence of covariates in dichotomous variables or a 1 SD increase in continuous variables.
CI = confidence interval; OR = odds ratio; other abbreviations as in Table 1.

JACC: CARDIOVASCULAR IMAGING, VOL. 3, NO. 9, 2010
SEPTEMBER 2010:908–17

Table 3. Associations With the Presence and Extent of NCP

	Presence				Extent			
	Univariate		Multivariate		Univariate		Multivariate	
	OR (95% CI)*	p Value	OR (95% CI)*	p Value	OR (95% CI)†	p Value	OR (95% CI)†	p Value
Age, per 11 yrs	1.21 (1.00–1.47)	0.05	1.45 (1.15–1.86)	0.002	1.28 (1.06–1.57)	0.01	1.53 (1.20–1.97)	0.0007
Sex, men	3.04 (2.02–4.59)	<0.0001	2.37 (1.44–3.91)	0.0007	2.42 (1.60–3.70)	<0.0001	1.85 (1.11–3.10)	0.02
VAT, per 58 cm^2	2.13 (1.71–2.82)	<0.0001	1.68 (1.28–2.22)	0.0002	1.74 (1.41–2.18)	<0.0001	1.31 (1.03–1.68)	0.03
Hypertension	2.18 (1.46–3.25)	0.0001	1.34 (0.85–2.11)	0.20	3.13 (2.08–4.79)	<0.0001	2.31 (1.46–3.68)	0.0004
Hypercholesterolemia	2.35 (1.59–3.52)	<0.0001	2.00 (1.28–3.14)	0.002	1.65 (1.12–2.44)	0.01	1.48 (0.95–2.30)	0.08
Diabetes mellitus	2.03 (1.36–3.04)	0.0005	1.61 (1.02–2.55)	0.04	2.63 (1.78–3.92)	<0.0001	2.36 (1.52–3.70)	0.0001
Current smoking	2.93 (1.91–4.57)	<0.0001	2.22 (1.33–3.74)	0.002	2.42 (1.62–3.64)	<0.0001	1.95 (1.21–3.19)	0.007

*Odds ratio (95% confidence interval) for the presence of NCP associated with the presence of covariates in dichotomous variables or a 1-SD increase in continuous variables; †odds ratio (95% confidence interval) for high NCP counts (≥2; n = 177) versus low counts (≤ 1; n = 250).
NCP = noncalcified coronary plaque; other abbreviations as in Tables 1 and 2.

factors such as hypertension, hypercholesterolemia, diabetes mellitus, and current smoking, increased VAT area (per 1 SD, 58 cm^2) was significantly associated with both the presence (odds ratio [OR]: 1.68; 95% confidence interval [CI]: 1.28 to 2.22) and extent (OR: 1.31; 95% CI: 1.03 to 1.68) of NCP. Age- and sex-adjusted Pearson's correlations between adiposity measurements are provided in Table 4. Despite the positive correlations that were found between these variables, only VAT remained an independent predictor of the presence and extent of NCP after adjustment for clinical variables (Table 5). Further adjustment for BMI, waist circumference, and subcutaneous adipose tissue area did not change the significant association of VAT with NCP (presence: OR: 1.79; 95% CI: 1.25 to 2.83, extent: OR: 1.56; 95% CI: 1.08 to 2.29). Table 6 shows the results of age- and sex-adjusted and multivariate analyses of the association between VAT and vulnerable NCP characteristics. Increased VAT area was independently associated with the presence of NCP with PR, low CT density, and adjacent spotty calcium.

DISCUSSION

In the present study, we show that VAT area is significantly associated with the presence and extent of NCP, as detected by 64-slice CTA. This association is independent of traditional coronary risk factors. Taken together with our previous reports (6), the present data indicate that visceral adiposity is associated with a higher likelihood of having CAD and, if present, more diffuse CAD compared with patients without visceral adiposity. Importantly, the study also demonstrates that high VAT area is significantly associated with the presence of NCP with PR, low CT density, and spotty calcium, which may represent vulnerable characteristics, as previously described (9,11,12). Thus, our data suggest that the accumulation of VAT may contribute to the acceleration of atherosclerosis and to plaque vulnerability.

Association between VAT area and coronary plaque burden in 64-slice CTA. We have previously reported that the accumulation of VAT is an independent predictor of the presence and extent of CAC detected by multidetector CT (6). Although several epidemiological studies have been done, there is a paucity of data regarding direct associations between VAT and the distribution of NCP. Whereas the quantification of CAC is considered to provide prognostic information (17), a recent CTA study suggested that the number of NCPs with a calcified component (namely, mixed plaques) was an independent predictor of acute cardiac events (18). In the present study, we found a positive association between VAT accumulation and NCP burden using 64-slice CTA. These findings may have important therapeutic implications because information about the plaque burden determined by CTA may help to identify patients with visceral adiposity at high risk for cardiovascular events. The identification of such patients is essential to initiate aggressive therapeutic strategies, such as lifestyle modification and pharmacological interventions.

Table 4. Age- and Sex-Adjusted Pearson's Correlation Coefficients

	VAT	SAT	BMI	WC
VAT	—			
SAT	0.53	—		
BMI	0.65	0.70	—	
WC	0.77	0.79	0.77	—

p < 0.0001 for all correlations. Abbreviations as in Table 1.

Table 5. Associations of Adiposity Measurements With the Presence and Extent of NCP

	Presence				Extent			
	Univariate		Multivariate*		Univariate		Multivariate*	
	OR (95% CI)†	p Value	OR (95% CI)†	p Value	OR (95% CI)‡	p Value	OR (95% CI)‡	p Value
VAT (per 58 cm^2)	2.13 (1.71–2.82)	<0.0001	1.68 (1.28–2.22)	0.0002	1.74 (1.41–2.18)	<0.0001	1.31 (1.03–1.68)	0.03
SAT (per 65 cm^2)	0.82 (0.67–1.00)	0.04	0.97 (0.77–1.23)	0.8	0.84 (0.68–1.02)	0.08	0.96 (0.75–1.22)	0.7
BMI (per 3.5 kg/m^2)	1.13 (0.94–1.37)	0.2	1.02 (0.81–1.28)	0.9	1.08 (0.89–1.32)	0.4	0.96 (0.76–1.21)	0.7
WC (per 9.6 cm)	1.37 (1.13–1.69)	0.002	1.25 (0.99–1.58)	0.06	1.23 (1.02–1.50)	0.03	1.08 (0.86–1.37)	0.5

*Adjusted for age, sex, hypertension, hypercholesterolemia, diabetes mellitus, and current smoking; †odds ratio (95% confidence interval) for the presence of NCP associated with a 1 − SD increase in adiposity measurements. ‡Odds ratio (95% confidence interval) for high NCP counts (≥2; n = 177) versus low counts (≤1; n = 250).
NCP = noncalcified coronary plaque; other abbreviations as in Tables 1 and 2.

Recent studies have suggested that increased epicardial adipose tissue (19) or low levels of adiponectin (20) are more associated with NCP rather than calcified plaque. In accordance with these results, we found that VAT had stronger association with NCP (OR: 1.68, p = 0.0002) than with calcified plaque (OR: 1.34, p = 0.02). These findings may suggest that release of inflammatory adipocytokines from VAT may sustain an active atherosclerotic process as proven by the presence of NCP. The presence of mere CAC (calcified plaque), instead, could represent a more advanced and stable phase of the atherosclerotic disease process.

The present data suggest that VAT accumulation accelerates atherosclerosis independently of traditional cardiovascular risk factors such as hypertension, hypercholesterolemia, and diabetes. These observations may contribute to our understanding that nontraditional risk factors such as hyperinsulinemia and elevated apolipoprotein B and small low-density lipoprotein particles, which are commonly found in patients with visceral adiposity, may increase the risk of CAD beyond that predicted by the presence of traditional risk factors (21). Notably, the odds ratios for NCP were higher with smoking than with VAT in a multivariate model, suggesting that smoking may facilitate the accumulation of VAT. Taking into account a previous report that smoking habits are independently related to VAT (22), smoking may confound the relationship between VAT and CAD risk.

BMI was not significantly associated with NCP in the present study. We also found that BMI and VAT area were only moderately related, indicating that BMI and VAT convey different information. Interestingly, we found that subcutaneous adipose tissue was protective against NCP in univariate analyses, which may confirm previous results that subcutaneous adiposity has favorable effects on CAD (4).

Association between VAT area and the vulnerability of NCP. Several epidemiological studies have suggested that visceral adiposity is linked to the development of acute coronary syndrome (ACS) (4,5). However, the association between visceral adiposity and coronary plaque vulnerability is unclear. Several prior CTA studies have shown that NCP is associated, more so than calcified coronary plaque, with the occurrence of ACS (9). Moreover, we previously documented that PR, low CT density, and adjacent spotty calcium represent CTA-detected plaque vulnerability (12). In the present study, using 64-slice CTA, we provide definitive evidence for increased coronary plaque vulnerability in patients with visceral adiposity.

Although there are many pathways by which visceral adiposity is causally linked to atherosclerosis, 1 possible mechanism is that adipocytokines secreted from VAT, including tumor necrosis factor-α, IL-6, free fatty acids, adiponectin, and plasminogen activator-1, may directly influence the vessel wall atherogenic environment by regulating gene expression and the function of endothelial and arterial smooth muscle, and macrophage cells (23). For example, insulin resistance, which is promoted by free fatty acids, is thought to increase atherogenesis and atherosclerotic plaque instability by inducing proinflammatory activity in vas-

Table 6. Relationship Between VAT and NCP Characteristics in CT Angiography

	Age- and Sex-Adjusted		Multivariate*	
	OR (95% CI)†	p Value	OR (95% CI)†	p Value
Positive remodeling	2.00 (1.57–2.57)	<0.0001	1.71 (1.18–2.53)	0.005
Low CT density	1.66 (1.33–2.11)	<0.0001	1.69 (1.17–2.47)	0.006
Spotty calcium	1.69 (1.34–2.17)	<0.0001	1.52 (1.03–2.27)	0.04
All 3 characteristics	1.89 (1.47–2.54)	<0.0001	1.58 (1.05–2.41)	0.03

*Adjusted for age, sex, BMI, SAT, WC, hypertension, hypercholesterolemia, diabetes mellitus, and current smoking; †odds ratio (95% confidence interval) for the presence of each CT characteristic per 1 − SD (58 cm^2) increase in VAT.
CT = computed tomography; NCP = noncalcified coronary plaque; other abbreviations as in Tables 1 and 2.

cular and immune cells (24). Furthermore, increased levels of plasminogen activator-1 can inhibit plasminogen-induced migration and proliferation of vascular smooth muscle cells, leading to the formation of plaques with thin fibrous caps, necrotic cores, and rich in macrophages that are prone to rupture (25).

Taken together, our findings may partially explain the excess cardiovascular risk in patients with visceral adiposity, suggesting that excess VAT accumulation is associated with a proinflammatory metabolic profile that is predictive of an unstable atherosclerotic plaque. Therefore, stabilization of the atherosclerotic plaque may offer a legitimate therapeutic target to reduce the risk of ACS in patients with visceral adiposity.

Study limitations. First, although our data support the notion that VAT is an important factor in the pathogenesis of atherosclerosis, causality cannot be established because this is a cross-sectional study. Prospective and larger population studies are needed to elucidate whether the occurrence of CTA-detected vulnerable NCPs, in combination with increased VAT area, might help to identify patients at high risk for cardiovascular events. Second, the study population comprised patients with proven or suspected CAD; thus, our results do not apply to patients with a lower probability of CAD. Third, inflammatory markers were not measured in the present study. The previous article (26) demonstrates that epicardial adipose tissue in patients with critical CAD has higher expressions of inflammatory mediators compared with their subcutaneous adipose tissue. Further studies are needed to clarify which inflammatory markers mediate the association between VAT and atherosclerosis. Finally, the current appropriate clinical guidelines do not recommend screening with CTA because of the high radiation exposure, the use of contrast agents, cost effectiveness and limited evidence (27). However, investigational studies using CTA should be encouraged to better understand the role of detecting the plaque burden and vulnerability in patients with visceral adiposity, which may help improve risk prediction and the prevention of such events.

CONCLUSIONS

We have demonstrated that increased VAT is significantly associated with the presence, extent, and vulnerable characteristics of NCPs, as assessed by 64-slice CTA. Our findings support the hypothesis that the accumulation of VAT may contribute to the progression and instability of coronary atherosclerotic plaques. Long-term studies of the cardiovascular event risk in patients with visceral adiposity are important, and 64-slice CTA may offer an approach to improve risk stratification in such patients.

Reprint requests and correspondence: Dr. Hideya Yamamoto, Department of Cardiovascular Medicine, Graduate School of Biomedical Sciences, Hiroshima University, 1-2-3 Kasumi Minami-ku, Hiroshima 734-8551, Japan. *E-mail: hideyayama@hiroshima-u.ac.jp.*

REFERENCES

1. Manson JE, Colditz GA, Stampfer MJ, et al. A prospective study of obesity and risk of coronary heart disease in women. N Engl J Med 1990;322:882–9.
2. Kissebah AH, Vydelingum N, Murray R, et al. Relation of body fat distribution to metabolic complications of obesity. J Clin Endocrinol Metab 1982;54:254–60.
3. Després JP, Moorjani S, Lupien PJ, Tremblay A, Nadeau A, Bouchard C. Regional distribution of body fat, plasma lipoproteins, and cardiovascular disease. Arteriosclerosis 1990;10:497–511.
4. Yusuf S, Hawken S, Ounpuu S, et al. Obesity and the risk of myocardial infarction in 27,000 participants from 52 countries: a case-control study. Lancet 2005;366:1640–9.
5. Nicklas BJ, Penninx BW, Cesari M, et al. Association of visceral adipose tissue with incident myocardial infarction in older men and women: the Health, Aging and Body Composition Study. Am J Epidemiol 2004;160:741–9.
6. Ohashi N, Yamamoto H, Horiguchi J, et al. Visceral fat accumulation as a predictor of coronary artery calcium as assessed by multislice computed tomography in Japanese patients. Atherosclerosis 2009;202:192–9.
7. Yamagishi M, Terashima M, Awano K, et al. Morphology of vulnerable coronary plaque: insights from follow-up of patients examined by intravascular ultrasound before an acute coronary syndrome. J Am Coll Cardiol 2000;35:106–11.
8. Varnava AM, Mills PG, Davies MJ. Relationship between coronary artery remodeling and plaque vulnerability. Circulation 2002;105:939–43.
9. Motoyama S, Kondo T, Sarai M, et al. Multislice computed tomographic characteristics of coronary lesions in acute coronary syndromes. J Am Coll Cardiol 2007;50:319–26.
10. Leber AW, Becker A, Knez A, et al. Accuracy of 64-slice computed tomography to classify and quantify plaque volumes in the proximal coronary system: a comparative study using intravascular ultrasound. J Am Coll Cardiol 2006;47:672–7.
11. Kitagawa T, Yamamoto H, Ohhashi N, et al. Comprehensive evaluation of non-calcified coronary plaque characteristics detected using 64-slice computed tomography in patients with proven or suspected coronary artery disease. Am Heart J 2007;154:1191–8.

12. Kitagawa T, Yamamoto H, Horiguchi J, et al. Characterization of noncalcified coronary plaques and identification of culprit lesions in patients with acute coronary syndrome by 64-slice computed tomography. J Am Coll Cardiol Cardiovasc Imaging 2009;2:153–60.
13. Nathan DM, Balkau B, Bonora E, et al. International Expert Committee report on the role of the A1C assay in the diagnosis of diabetes. Diabetes Care 2009;32:1327–34.
14. Teramoto T, Sasaki J, Ueshima H, et al. Executive summary of Japan Atherosclerosis Society (JAS) guideline for diagnosis and prevention of atherosclerotic cardiovascular diseases for Japanese. J Atheroscler Thromb 2007;14:45–50.
15. Agatston AS, Janowitz WR, Hildner FJ, et al. Quantification of coronary artery calcium using ultrafast computed tomography. J Am Coll Cardiol 1990;15:827–32.
16. Kajinami K, Seki H, Takekoshi N, Mabuchi H. Coronary calcification and coronary atherosclerosis: site by site comparative morphologic study of electron beam computed tomography and coronary angiography. J Am Coll Cardiol 1997;29:1549–56.
17. Budoff MJ, Shaw LJ, Liu ST, et al. Long-term prognosis associated with coronary calcification: observations from a registry of 25,253 patients. J Am Coll Cardiol 2007;49:1860–70.
18. Pundziute G, Schuijf JD, Jukema JW, et al. Prognostic value of multislice computed tomography coronary angiography in patients with known or suspected coronary artery disease. J Am Coll Cardiol 2007;49:62–70.
19. Alexopoulos N, McLean DS, Janik M, Arepalli CD, Stillman AE, Raggi P. Epicardial adipose tissue and coronary artery plaque characteristics. Atherosclerosis 2010;210:150–4.
20. Broedl UC, Lebherz C, Lehrke M, et al. Low adiponectin levels are an independent predictor of mixed and non-calcified coronary atherosclerotic plaques. PLoS One 2009;4:e4733.
21. Lamarche B, Tchernof A, Mauriège P, et al. Fasting insulin and apolipoprotein B levels and low-density lipoprotein particle size as risk factors for ischemic heart disease. JAMA 1998;279:1955–61.
22. Seidell JC, Cigolini M, Deslypere JP, Charzewska J, Ellsinger BM, Cruz A. Body fat distribution in relation to physical activity and smoking habits in 38-year-old European men. The European Fat Distribution Study. Am J Epidemiol 1991;133:257–65.
23. Fantuzzi G, Mazzone T. Adipose tissue and atherosclerosis: exploring the connection. Arterioscler Thromb Vasc Biol 2007;27:996–1003.
24. Kappert K, Meyborg H, Clemenz M, et al. Insulin facilitates monocyte migration: a possible link to tissue inflammation in insulin-resistance. Biochem Biophys Res Commun 2008;365:503–8.
25. Hajer GR, van Haeften TW, Visseren FL. Adipose tissue dysfunction in obesity, diabetes, and vascular diseases. Eur Heart J 2008;29:2959–71.
26. Mazurek T, Zhang L, Zalewski A, et al. Human epicardial adipose tissue is a source of inflammatory mediators. Circulation 2003;108:2460–6.
27. Bluemke DA, Achenbach S, Budoff M, et al. Noninvasive coronary artery imaging: magnetic resonance angiography and multidetector computed tomography angiography: a scientific statement from the American Heart Association Committee on cardiovascular imaging and intervention of the council on cardiovascular radiology and intervention, and the Councils on Clinical Cardiology and cardiovascular disease in the young. Circulation 2008;118:586–606.

Key Words: 64-slice computed tomography angiography ■ noncalcified coronary plaque ■ plaque vulnerability ■ visceral adipose tissue.

Journal of Digital Imaging

Is It Possible to Predict Heart Rate and Range during Enhanced Cardiac CT Scan from Previous Non-enhanced Cardiac CT?

Jun Horiguchi,[1,2,7] Hideya Yamamoto,[3] Ryuichi Arie,[4] Masao Kiguchi,[1] Chikako Fujioka,[1] Megu Ohtaki,[5] Yasuki Kihara,[3] and Kazuo Awai[6]

The effect of heart rate and variation during cardiac computed tomography (CT) on the examination quality. The purpose of this study is to investigate whether it is possible to predict heart rate and range during enhanced cardiac computed CT scan from previous non-enhanced cardiac CT scan. Electrocardiograph (ECG) files from 112 patients on three types of cardiac 64-slice CT (non-enhanced, prospective ECG-triggered and retrospective ECG-gated enhanced scans) were recorded. The mean heart rate, range (defined as difference between maximal and minimal heart rates) and the range ratio (defined as maximal heart rate divided by minimal heart rate) during the scans were compared. Scan time was 4.8, 4.6, and 7.3 s on non-enhanced, prospective ECG-triggered and retrospective ECG-gated scans, respectively ($p<0.0001$). The heart rates were not significantly different (60±9 beats per minute (bpm), 60±9 and 61±10 bpm; $p = 0.64$). Heart rate on the enhanced scan markedly correlated with that of the non-enhanced scan ($r = 0.78$ and 0.74). In contrast, the ranges of heart rate were 2±5, 4±8, and 8± 21 bpm, with different range ratios (1.04, 1.07, and 1.14; $p<0.0001$). Correlation of heart rate ranges between non-enhanced scan versus prospective ECG-triggered scan was low ($r = 0.27$) and that between non-enhanced scan versus retrospective ECG-gated scan negligible ($r = -0.027$).Heart rate on enhanced cardiac CT, in most cases, can be predicted from a non-enhanced scan. Heart rate range on enhanced cardiac CT, however, is hard to predict from the non-enhanced scan.

KEY WORDS: Cardiac, computed tomography, heart rate, heart rate range

INTRODUCTION

Image quality and detection of stenosis in coronary computed tomography (CT) angiography (CTA) is affected by heart rate and the range during acquisition.[1–6] With single-source 64-slice CTA, most investigators recommend lowering the patient's heart rate to <65 beats per minute (bpm) to achieve stable image quality.[7–10] In this range, diagnostic image quality can be obtained for all coronary arteries at a single reconstruction interval at mid-diastole.[11] When higher heart rates are included however, additional reconstructions at late systole may be required for optimal visualization of the right coronary artery.[12] The variation of heart rate alters the data acquisition window of the cardiac cycle, which may result in the inclusion of systole. In order to reduce and stabilize the heart

[1]*From the Department of Clinical Radiology, Hiroshima University Hospital, 1-2-3, Kasumi-cho, Minami-ku, Hiroshima 734-8551, Japan.*

[2]*From the Department of Radiology, Hiroshima Kyoritsu Hospital, 2-19-6, Nakasu, Asaminami-ku, Hiroshima 731-0121, Japan.*

[3]*From the Department of Cardiovascular Medicine, Hiroshima University Graduate School of Biomedical Sciences and Hiroshima University Hospital, 1-2-3, Kasumi-cho, Minami-ku, Hiroshima 734-8551, Japan.*

[4]*From the Department of Radiology, Chuden Hospital, 3-4-27, Oote-machi, Naka-ku, Hiroshima 730-8562, Japan.*

[5]*From the Department of Environmetrics and Biometrics, Research Institute for Radiation Biology and Medicine, Hiroshima University, 1-2-3, Kasumi-cho, Minami-ku, Hiroshima 734-8551, Japan.*

[6]*From the Division of Medical Intelligence and Informatics, Programs for Applied Biomedicine, Graduate School of Biomedical Sciences, Department of Radiology, Hiroshima University, 1-2-3, Kasumi-cho, Minami-ku, Hiroshima 734-8551, Japan.*

[7]*From the 2-19-6, Nakasu, Asaminami-ku, Hiroshima 731-0121, Japan.*

Correspondence to: Jun Horiguchi, 2-19-6, Nakasu, Asaminami-ku, Hiroshima 731-0121, Japan; tel: +81-82-8791111; e-mail: horiguchi@hiroshimairyo.or.jp

doi: 10.1007/s10278-010-9333-2

Published online: 08 September 2010

rate, β-blocker is often used on cardiac CT, administered orally at 1 to 2 h(s) prior to the examination or/and intravenously just before the examination.

Practitioners have to decide the acquisition protocol depending on the heart rate. electrocardiograph (ECG) editing; i.e., by arbitrarily modifying the position of the temporal windows within the cardiac cycle, to correct and compensate for part or all of the artifacts,[13] is not perfect but is the most robust imaging technique for instable heart rates. As it needs retrospective ECG-gated CTA without ECG-correlated tube current modulation however, it involves a high radiation dose. In patients with a relatively stable heart rate, ECG-correlated tube current modulation, reducing radiation exposure by 30% to 50%, is used.[14,15] In this technique, the practitioner has to determine the peak current interval relative to the cardiac phase and the minimal current value relative to the maximal current. Recently devised prospective ECG-triggered coronary 64-slice CTA[16] needs low and stable heart rate.[17]

In these circumstances, prediction of heart rate and variation is important on 64-slice CTA for deciding use of β-blockers and the determination of scanning protocol. The purpose of this study is to investigate whether it is possible to predict heart rate and range during enhanced cardiac CT from non-enhanced cardiac CT.

MATERIALS AND METHODS

Patients

The comparative study between prospective ECG-triggered and retrospective ECG-gated cardiac 64-slice CTA[18] was approved by the local hospital ethics committee and all patients provided written informed consent. This study analyzed heart rate and heart rate range of 112 patients (63 males and 49 females, 64±11 years old: ranged, 35–87 years) undergoing coronary artery calcium scoring and two types of coronary CTA. The mean body mass index was 24±13 kg/m^2. Of 112 patients, 87 (78%) were symptomatic and 71 (64%) had coronary risk factors. Using a 64-slice CT scanner (Lightspeed VCT, GE Healthcare, Waukesha, WI), 86 patients were scanned with retrospective ECG-gated CTA first, followed by prospective ECG-triggered CTA and the remaining 26 patients were scanned in reverse order. The time interval between the two scans was 5 min. To minimize motion artifacts, patients with an initial heart rate ≥60 bpm (n=83) were given with oral β-blocker (metoprolol 40 mg) to achieve a target heart rate of 50–60 bpm. No additional intravenous β-blocker, at the time of the examination, was used. Except for two patients with contraindications, nitroglycerin spray (one push, Mycor spray, Astellas pharma, Tokyo, Japan) was used 5 min before coronary CTA scan to dilate the diameters of the coronary arteries.[19]

Data Acquisition

Each scan was performed 5 s after breath-hold at mild-inspiration in order to minimize range of heart rate, which was investigated on non-enhanced cardiac CT.[20] The ECG files were obtained using three lead ECG during the CT scan, and the data were transferred to an external PC for further analysis.

The use of contrast media included 10 ml Iopamiron® 370 (Bayer-Schering Pharma, Berlin, Germany), followed by 25 ml saline chaser for test bolus scan and contrast media (volume=body weight (in kg)×0.6 ml), followed by 25 ml saline chaser for each type of coronary CTA. The injection rate of contrast media and saline was 0.06×body weight ml/s (the contrast media was administered during 10 s).

Patients with atrial fibrillation and having beat-to-beat variability exceeding 20 bpm during pre-examination baseline breathing were excluded from analysis.[21] This was because such types of heartbeat might disturb the analysis of the effect of contrast media or scan time on heart rate.

Electrocardiograph Data Evaluation and Statistical Analysis

Mean heart rate, the range (defined as difference between maximal and minimal heart rates) and the range ratio (defined as maximal heart rate divided by minimal heart rate) during scanning were compared between the three scans. Depending on the data distribution, one-factor analysis of variance (ANOVA) or Kruskal–Wallis was used.

Mean heart rate and the range on prospective ECG-triggered and retrospective ECG-gated enhanced scans in relation to the non-enhanced scan were tested using Pearson's correlation coefficient and Bland–Altman analysis with a 95% confidence interval (CI). The degree of Pearson's product moment correlation coefficient (r) was regarded as follows: 0 to 0.2, no or negligible; 0.2 to 0.4, low; 0.4 to 0.6, moderate; 0.6 to 0.8, marked and 0.8 to 1.0, high. Student's t test was used to determine the difference in acquisition time, heart rate, and the range between two groups divided by scan order. P values <0.05 were considered to identify significant differences.

RESULTS

All patients were able to hold their breath on the three scans. All scans were performed without any significant adverse effect of contrast material. The data acquisition time was 4.8±1.1 s (median, 4.7 s; 95% CI, 4.5 and 4.9 s) in non-enhanced scan, 4.6±1.2 s (median, 4.5 s; 95% CI, 4.2 and 4.8 s) in prospective ECG-triggered scan and 7.3±1.0 s (median, 7.2 s; 95% CI, 7.0 and 7.3 s) in retrospective ECG-gated scan (Kruskal–Wallis test; $p<0.01$). The data acquisition time was not different between two groups divided by scan order in non-enhanced, prospective ECG-triggered and retrospective ECG-gated scans ($p=0.23$, 0.64, and 0.47). The body weight was 62±14 (38–103) kg, and the total contrast volumes (test bolus scan, prospective ECG-triggered, and retrospective ECG-gated CTA) administered was 85±16 (56–134) ml. The effective radiation dose, estimated based on the dose-length product, was 0.9±0.2, 4.1±1.8, and 19.8±3.5 mSv in non-enhanced, prospective ECG-triggered and retrospective ECG-gated scans, respectively.

Heart Rate

Heart rates were not significantly different between non-enhanced scan (60±9 bpm), prospective ECG-triggered scan (60±9 bpm), and retrospective ECG-gated scan (61±10 bpm; one-factor ANOVA; $p=0.64$). Heart rates markedly correlated between non-enhanced scan versus prospective ECG-triggered scan ($r=0.78$ (95% CI, 0.70 and 0.85); $p<0.01$) and non-enhanced scan versus retrospective ECG-gated scan ($r=0.74$ (95% CI; 0.64 and 0.81); $p<0.01$) (Fig. 1). Results in the Bland–Altman analysis are shown Table 1.

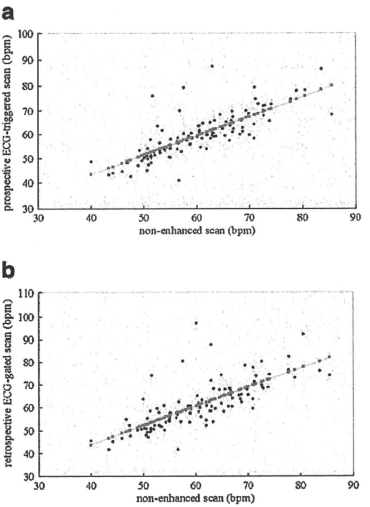

Fig 1. Scatterplots of heart rate between non-enhanced scan and enhanced scan a HR (prospective ECG-triggered scan) = 0.804×HR (non-enhanced scan) + 11.2 ($p<0.00001$; $r=0.78$ (95% CI, 0.70 and 0.85)); b HR (retrospective ECG-gated scan) = 0.840×HR (non-enhanced scan) + 10.2 ($p<0.00001$; $r=0.74$ (95% CI, 0.64 and 0.81)) HR = heart rate.

The heart rate was not different between two groups divided by scan order in non-enhanced, prospective ECG-triggered and retrospective ECG-gated scans ($p=0.46$, 0.25, and 0.17).

Heart Rate Range

Heart rate ranges were non-enhanced scan: 2±5 bpm (median, 1.3 bpm; 95% CI, 1.1 and 1.6 bpm), prospective ECG-triggered scan: 4±8 bpm (median, 2.1 bpm; 95% CI, 1.7 and 2.5 bpm), and retrospective ECG-gated scans: 8±21 bpm (median, 2.7 bpm; 95% CI, 2.2 and 3.2 bpm), with different heart rate range ratios (1.04, 1.07, and 1.14, Kruskal–Wallis test; $p<0.00001$). The heart rate range >5 bpm occurred in 5.4% (6/112), 8.9% (10/112) and 20.5% (23/112) in

Table 1. Non-enhanced Scan versus Prospective Scan and Non-enhanced Scan Versus Retrospective Scan

	Non-enhanced	Prospective	Retrospective	Non-enhanced versus prospective		Non-enhanced versus retrospective	
	Mean ± SD	Mean ± SD	Mean ± SD	Bias	Limits of agreement	Bias	Limits of agreement
Heart rate (bpm)	60.5 ± 9.1	59.8 ± 9.3		0.6	−11.3 to 12.6		
Heart rate range (bpm)	2.3 ± 4.7	3.9 ± 7.9		−0.5	−14.5 to 13.4		
Heart rate (bpm)	60.5 ± 9.1		61.0 ± 10.3			−1.6	−17.4 to 14.2
Heart rate range (bpm)	2.3 ± 4.7		8.2 ± 21.0			−5.9	−48.5 to 36.4

Non-enhanced and enhanced scans were compared using Bland–Altman analysis
SD standard deviation

non-enhanced, prospective ECG-triggered and retrospective ECG-gated scans, respectively. Similarly, the heart rate range >10 bpm occurred in 4.5% (5/112), 7.1% (8/112), and 11.6% (13/112). Correlation of heart rate ranges between non-enhanced scan versus prospective ECG-triggered scan was low (r=0.27 (95% CI, 0.09 and 0.43)) and that between non-enhanced scan versus retrospective ECG-gated scan negligible (r=−0.027 (95% CI, −0.21 and 0.16)) (Fig. 2). Results in the Bland–Altman analysis are shown Table 1. In summary, marked degree of range occurred in both enhanced and non-enhanced scans. Marked range in non-enhanced scan does not predict the same during enhanced scanning and vice versa. The heart rate range was not different between the two groups divided by scan order in non-enhanced, prospective ECG-triggered and retrospective ECG-gated scans (p=0.18, 0.70, and 0.24).

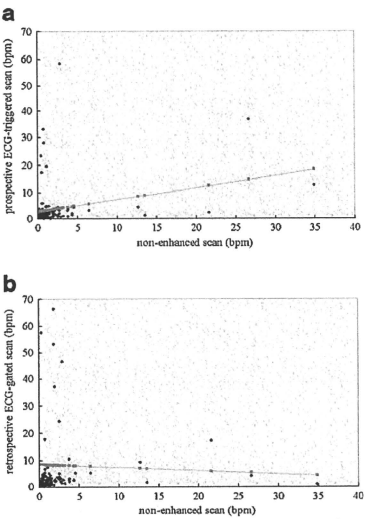

Fig 2. Scatterplots of heart rate range between non-enhanced scan and enhanced scan a HR range (prospectiveECG-triggered scan) = 0.285×HR range (non-enhanced scan) + 2.8 (p<0.01; r = 0.27 (95% CI, 0.09 and 0.43)); b HR range (retrospective ECG-gated scan) = −0.118×HR range (non-enhanced scan) + 8.48 (p = 0.781; r = −0.027 (95% CI, −0.21 and 0.16)) HR = heart rate.

DISCUSSION

This study compares heart rate and range between non-enhanced scan and enhanced scans with two data acquisition times. The results of our study suggest that (1) heart rate on enhanced cardiac CT, in most cases, can be predicted from a non-enhanced scan, (2) heart rate range on enhanced cardiac CT is not relevant to non-enhanced scan and is greater than non-enhanced scan, (3) a shorter scan time is advantageous for reducing heart rate range.

We found one previous study by Zhang et al., using relatively longer scan times (13–14 s for non-enhanced and enhanced scans), examining heart rate and range.[21] They showed that injection of contrast media had no significant effect on heart rate, which is in line with our study. They showed that percentage of beats outside a ±5 bpm about the mean was not different between non-enhanced (3.0%) and enhanced (3.3%) scans. In contrast to this, our results showed greater heart rate range on the enhanced scan compared with the non-enhanced scan. The reason for the difference is

not clear; however, we consider that greater heart rate range on the enhanced scan may be explained by the influence of increased venous return associated with bolus injection, the effect of iodine and psychological reaction.

Possible greater heart rate range with a longer scan time seems to be understandable. For 64-slice CT, a typical scan time required to image the heart is approximately 5–15 s, depending on CT scanner model.[21] A relatively shorter scan time of the CT scanner we used, is likely to offer small heart rate range. Recently, next-generation 320-detector row CT, enabling full heart coverage in one cardiac cycle, has been announced. This technology has a definite advantage in terms of heart rate range.

We would like to emphasize the importance of non-enhanced CT. Compared with non-enhanced scan for calcium scoring, coronary CTA uses higher radiation dose, especially with retrospective ECG-gating algorithm. The scan coverage is set up visually on the topogram; however, the position of the scanning start can vary according to individual anatomy.[22] To avoid repeated scan, there is a tendency to expose tissues beyond the boundaries of the volume to be imaged. Therefore, optimization of scan coverage from non-enhanced CT scan data is important. In addition, one must be aware that the quality of the CTA is likely to be impaired or non-diagnostic if large quantities of coronary calcium are found on non-enhanced CT.[23,24] Thus as mentioned above, apart from ECG information, we need get the most out of non-enhanced prior to coronary CTA.

We acknowledge the following limitation to our study. Enhanced scans were performed twice, and the numbers of patient were not the same level between two types of scan order. The effect of previously injected contrast is not negligible although this is likely to be minimized after the scan interval of 5 min. The fact that the patient was aware of what is going to happen to them for the second of the contrast studies might lead them less anxious.

In conclusion, the results suggest that heart rate on enhanced cardiac CT, in most cases, can be predicted from the non-enhanced scan. This is useful for determining protocol, i.e., helical or axial scan and the pitch in case of helical scan. In contrast, heart rate range in enhanced scan is greater than non-enhanced scan and is hard to predict from non-enhanced scan. In this respect, a shorter scan time has a definite advantage.

ACKNOWLEDGEMENTS

This study was financially supported by Tsuchiya Foundation (http://www.tsuchiya-foundation.or.jp), Hiroshima, Japan.

REFERENCES

1. Kroft LJM, de Roos A, Geleijns J: Artifacts in ECG-synchronized MDCT coronary angiography. AJR 189:581–591, 2007

2. Herzog C, Arning-Erb M, Zangos S, et al: Multi-detector row CT coronary angiography: influence of reconstruction technique and heart rate on image quality. Radiology 238:75–86, 2006

3. Giesler T, Baum U, Ropers D, et al: Noninvasive visualization of coronary arteries using contrast-enhanced multidetector CT: influence of heart rate on image quality and stenosis detection. AJR 179:911–916, 2002

4. Wintersperger BJ, Nikolaou K, von Ziegler F, et al: Image quality, motion artifacts and reconstruction timing of 64-slice coronary computed tomography angiography with 0.33-second rotation speed. Invest Radiol 41:436–442, 2006

5. Caussin C, Larchez C, Ghostine S, et al: Comparison of coronary minimal lumen area quantification by 64-slice computed tomography versus intravascular ultrasound for intermediate stenosis. Am J Cardiol 98:871–876, 2006

6. Leschka S, Scheffel H, Husmann L, et al: Effect of decrease in heart rate variability on the diagnostic accuracy of 64-MDCT coronary angiography. AJR 190:1583–1590, 2008

7. Fine JJ, Hopkins CB, Ruff N, Newton FC: Comparison of accuracy of 64-slice cardiovascular computed tomography with coronary angiography in patients with suspected coronary artery disease. Am J Cardiol 97:173–174, 2006

8. Leber AW, Knez A, von Ziegler F, et al: Quantification of obstructive and nonobstructive coronary lesions by 64-slice computed tomography: a comparative study with quantitative coronary angiography and intravascular ultrasound. J Am Coll Cardiol 46:147–154, 2005

9. Raff GL, Gallagher MJ, O'Neill WW, Goldstein JA: Diagnostic accuracy of noninvasive coronary angiography using 64-slice spiral computed tomography. J Am Coll Cardiol 46:552–557, 2005

10. Achenbach S: Computed tomography coronary angiography. J Am Coll Cardiol 48:1919–1928, 2006

11. Leshka S, Husmann L, Desbiolles LM, et al: Optimal image reconstruction intervals for non-invasive coronary angiography with 64-slice CT. Eur Radiol 16:1964–1972, 2006

12. Ferencik M, Nomura CH, Maurovich-Horvat P, et al: Quantitative parameters of image quality in 64-slice computed tomography angiography of the coronary arteries. Eur J Radiol 57:373–379, 2006

13. Cademartiri F, Mollet NR, Runza G, et al: Improving diagnostic accuracy of MDCT coronary angiography in patients with mild heart rhythm irregularities using ECG editing. AJR 186:634–638, 2006

14. Jakobs TF, Becker CR, Ohnesorge B, et al: Multislice helical CT of the heart with retrospective ECG gating: reduction of radiation exposure by ECG-controlled tube current modulation. Eur Radiol 12:1081–1086, 2002

15. Hausleiter J, Meyer T, Hadamitzky M, et al: Radiation dose estimates from cardiac multislice computed tomography in daily practice: impact of different scanning protocols on effective dose estimates. Circulation 113:1305–1310, 2006

16. Hsieh J, Londt J, Vass M, Li J, Tang X, Okerlund D: Step-and-shoot data acquisition and reconstruction for cardiac X-ray computed tomography. Med Phys 33:4236–4248, 2006

17. Horiguchi J, Kiguchi M, Fujioka C, et al: Radiation dose, image quality, stenoses measurement and CT densitometry using prospective electrocardiograph-triggered coronary 64-MDCT angiography—a phantom study. AJR 190:315–320, 2008

18. Hirai N, Horiguchi J, Fujioka C, et al: Prospective electrocardiography-triggered versus retrospective electrocardiography-gated 64-slice coronary CT angiography: image quality, stenoses assessment and radiation dose. Radiology 248:424–430, 2008

19. Dewey M, Hoffmann H, Hamm B: Multislice CT coronary angiography: effect of sublingual nitroglycerine on the diameter of coronary arteries. Rofo 178:600–604, 2006

20. Horiguchi J, Shen Y, Hirai N, et al: Timing on 16-slice scanner and implications for 64-slice cardiac CT: do you start scanning immediately after breath-hold? Acad Radiol 13:173–176, 2006

21. Zhang J, Fletcher JG, Harmsen WS, et al: Analysis of heart rate and heart rate variation during cardiac CT examinations. Acad Radiol 15:40–48, 2008

22. Paul JF, Abada HT: Strategies for reduction of radiation dose in cardiac multislice CT. Eur Radiol 17:2028–2037, 2007

23. Stillman AE, Oudkerk M, Ackerman M, et al: Use of multidetector computed tomography for the assessment of acute chest pain: a consensus statement of the North American Society of Cardiac Imaging and the European Society of Cardiac Radiology. Eur Radiol 17:2196–2207, 2007

24. Liu X, Zhao X, Huang J, et al: Comparison of 3D free-breathing coronary MR angiography and 64-MDCT angiography for detection of coronary stenosis in patients with high calcium scores. AJR 189:1326–1332, 2007

International Journal of Cardiology xxx (2010) xxx–xxx

Contents lists available at ScienceDirect

International Journal of Cardiology

journal homepage: www.elsevier.com/locate/ijcard

Effects of statin therapy on non-calcified coronary plaque assessed by 64-slice computed tomography

Toshiro Kitagawa [a], Hideya Yamamoto [a,*], Jun Horiguchi [b], Norihiko Ohashi [a], Eiji Kunita [a], Hiroto Utsunomiya [a], Yasuki Kihara [a]

[a] Department of Cardiovascular Medicine, Graduate School of Biomedical Sciences, Hiroshima University, Hiroshima, Japan
[b] Department of Clinical Radiology, Hiroshima University Hospital, Hiroshima, Japan

ARTICLE INFO

Article history:
Received 22 October 2009
Received in revised form 5 February 2010
Accepted 7 March 2010
Available online xxxx

Keywords:
Statin
Lipid profile
Non-calcified atherosclerotic lesion
Computed tomography angiography

ABSTRACT

Computed tomography angiography (CTA) enables characterization of non-calcified coronary atherosclerotic lesions (NCALs) and assessment of plaque vulnerability. We investigated whether the characteristics of NCALs detected by 64-slice CTA were influenced by preceding statin therapy and serum lipid profiles.

Methods: Among 493 consecutive patients who underwent coronary CTA, we enrolled 114 patients with NCALs. We divided the patients into three groups according to preceding statin therapy: intensive statins (IS, $n=24$), moderate statins (MS, $n=26$), and no statin (NS, $n=64$). The vulnerability of each NCAL was evaluated by density (low-density plaque defined as CT density ≤ 38 HU), positive remodeling (remodeling index > 1.05), and the presence of adjacent spotty calcification.

Results: Percentages of patients in the IS, MS, and NS groups with low-density NCALs were 46%, 58%, and 80%, respectively ($p=0.009$) and positive remodeling NCALs were 54%, 58%, and 75%, respectively ($p=0.10$). We also found an inverse correlation between serum LDL-C level and the minimum plaque CT density. According to the regression equation, a CT density of 38 HU corresponded with LDL-C of 100 mg/dl. The number of low-density plaques was positively correlated with low-density to high-density lipoprotein cholesterol ratio (LDL-C/HDL-C). An LDL-C/HDL-C > 2.5 independently predicted multiple low-density plaques (OR 2.39 [95% CI: 1.28–4.86], $p<0.001$).

Conclusions: Our CTA findings demonstrate that low-density NCALs occur less frequently in patients with intensive statin pre-treatment. A high LDL-C/HDL-C ratio is also associated with larger numbers of low-density NCALs.

1. Introduction

Recent evidence suggests that lipid-lowering therapy reduces cardiovascular morbidity and mortality and causes regression of coronary atherosclerosis [1,2]. Serial studies using intravascular ultrasound (IVUS) show that regression of coronary atherosclerosis induced by intensive statin therapy is related to the large reduction in low-density lipoprotein cholesterol (LDL-C) [3–7]. Serial analysis with angioscopy demonstrates early loss of yellow color in plaques and IVUS volumetric analysis shows subsequent plaque regression in coronary artery disease patients treated with atorvastatin [7]. The benefits of intensive statin therapy may also be due to increased high-density lipoprotein cholesterol (HDL-C) [8].

Cardiac computed tomography (CT) identifies and characterizes non-calcified coronary atherosclerotic lesions (NCALs) *in vivo* [9–13]. We have previously reported that, in comparison with IVUS, 64-slice CT angiography (CTA) reliably assesses the components, vascular remodeling, and adjacent calcium morphology of NCALs. We have also found that lower CT densities, positive remodeling, and adjacent spotty coronary calcium frequently co-exist in potentially vulnerable lesions [12,13].

The relationship between the CTA characteristics of NCALs, statin therapy, and serum lipid profiles is of considerable interest. In the present study, we evaluated characteristics of NCALs assessed by 64-slice CTA after a period of statin therapy. We investigated the influence of lipid-lowering therapy on the characteristics of NCALs and whether the change in composition can be related to serum lipid levels.

2. Patients and methods

2.1. Subjects and study design

From December 2006 to March 2008, a total of 493 patients underwent coronary CTA at Hiroshima University Hospital. Exclusion criteria for the present study were acute coronary syndrome [14], previous percutaneous coronary intervention and/or

* Corresponding author. Department of Cardiovascular Medicine, Hiroshima University Graduate School of Biomedical Sciences, 1-2-3 Kasumi Minami-ku, Hiroshima 734-8551, Japan. Tel.: +81 82 257 5540; fax: +81 82 257 1569.
E-mail address: hideyayama@hiroshima-u.ac.jp (H. Yamamoto).

0167-5273/$ – see front matter © 2010 Elsevier Ireland Ltd. All rights reserved.
doi:10.1016/j.ijcard.2010.03.005

Please cite this article as: Kitagawa T, et al, Effects of statin therapy on non-calcified coronary plaque assessed by 64-slice computed tomography, Int J Cardiol (2010), doi:10.1016/j.ijcard.2010.03.005

coronary artery bypass surgery, missing serum examination at the period of CTA, uncertainty about medication use or preceding statin therapy of less than 6 months' duration, degraded image quality due to motion artifacts or inadequate contrast enhancement, and the absence of NCALs. We enrolled 114 patients with clinically proven or suspected coronary artery disease (86 men and 28 women, aged 67.6 ± 9.1 years). All patients had stable clinical presentation (no symptoms with an equivocal or positive cardiac stress test, or atypical chest pain, or stable exertional chest pain), and each underwent CTA for follow-up or diagnosis of coronary artery disease. The hospital ethics committee approved the study and we obtained written informed consent from all patients.

We measured fasting serum triglycerides, LDL-C, and HDL-C within 4 weeks of the CTA in all patients. We also calculated the LDL-C/HDL-C ratio. We recorded traditional coronary risk factors including hypertension (systolic/diastolic blood pressure ≥ 140/90 mm Hg, and/or current use of antihypertensive agents), diabetes mellitus (HbA1c level ≥ 6.5% and/or current use of hypoglycemic agents), and current smoking. We also noted the use of statins, angiotensin-converting enzyme inhibitors or angiotensin II receptor blockers (ACEI/ARB), and aspirin in the six months preceding the CTA. Patients were divided into three groups according to their statin use: intensive statins (IS, $n=24$), moderate statins (MS, $n=26$) and no statins (NS, $n=64$). Patients in the IS group were taking 10–20 mg of atorvastatin ($n=18$), 2.5–10 mg of rosuvastatin ($n=4$) or 2–4 mg of pitavastatin ($n=2$) and patients in the MS group were taking 10–20 mg of pravastatin ($n=24$) or 5–10 mg of simvastatin ($n=2$). We chose a treatment period of greater than six months based on a report regarding the effect of statin therapy on coronary lesions in Japan [3].

2.2. CTA scan protocol and reconstruction

We performed electrocardiographic-gated CTA using a 64-slice CT scanner (LightSpeed VCT, GE Healthcare, Little Chalfont, Buckinghamshire, UK) with a gantry rotation time of 0.35 s. Patients with a heart rate of ≥ 60 beats/min received 40 mg of oral metoprolol 60 min before scanning and all patients received 0.3 mg nitroglycerin sublingually just before scanning. We have previously described the scan protocol and reconstruction method [12]. In brief, after a plain scan to determine the calcium burden of the coronary tree and measure coronary calcium scores according to the standard Agatston method [15,16] (sequential scan with 16 × 2.5 mm collimation; tube current, 140 mA; tube voltage, 120 kV), we performed contrast-enhanced scanning using 30 to 50 ml (0.6–0.7 ml/kg) contrast medium (Iopamidol, 370 mg I/ml, Bayer Healthcare, Berlin, Germany) during an inspiratory breath-hold. Volume data sets were acquired in the helical mode (64 × 0.625 mm collimation; CT pitch factor, 0.18–0.24:1; tube current, 600–750 mA with ECG-modulation technique; tube voltage, 120 kV). The effective radiation dose was estimated based on the dose-length product and ranged from 15 to 18 mSv [12]. Image reconstruction was performed using image-analysis software (CardIQ™, GE Healthcare) on a dedicated computer workstation (Advantage Workstation Ver.4.2, GE Healthcare). A 'standard' kernel was used as the reconstruction filter. Either a half (temporal resolution = 175 ms) or a two-sector (temporal resolution < 175 ms) reconstruction algorithm was selected, and the optimal cardiac phase with the least motion artifacts was chosen individually.

2.3. Evaluation of NCAL characteristics

As previously described, we evaluated NCAL characteristics on CTA [12,13]. Two blinded and independent observers analyzed the CT image data set. All coronary segments > 2 mm in diameter were evaluated using curved multiplanar reconstruction images. Vessels were viewed in images reconstructed along the axis of the vessel of interest and in cross-sectional images perpendicular to the centerline of the vessel. We defined NCALs and coronary calcium as follows: NCAL, a low-density mass of > 1 mm^2 in size, located within the vessel wall and clearly distinguishable from the contrast-enhanced coronary lumen and the surrounding periarterial tissue; coronary calcium, a structure on the vessel wall with a CT density above that of the contrast-enhanced coronary lumen or with a CT density of > 120 Hounsfield units (HU) assigned to the coronary artery wall in a plain image. For NCAL and calcium analyses, the optimal image display setting was chosen on an individual basis; in general, the window was between 700 and 1000 HU and the level between 100 and 200 HU. We assessed NCAL vulnerability by determining the minimum CT density, the vascular remodeling index and adjacent calcium morphology, as previously described [12,13]. We assessed spotty type calcium deposits in or adjacent to each NCAL, defined as a calcium burden with a length less than 3/2 of the vessel diameter and a width less than 2/3 of the vessel diameter. Obstructive lesions were defined as ≥ 75% stenosis on CTA. Next, we determined the minimum CT density for each NCAL by placing at least 5 regions of interest (area = 1 mm^2) in each lesion and documenting the lowest value of these. We defined low-density NCALs as lesions with a minimum CT density of ≤ 38 HU [12]. We excluded any lesion with a CT density > 120 HU from the NCALs because of the high probability of calcified plaque [9]. We also measured coronary artery enhancement next to each NCAL by placing a region of interest (area = 1 mm^2) in the center of the coronary artery lumen as a reference. Finally, a remodeling index (RI) was determined by calculating the value of the maximal cross-sectional vessel area (mm^2) at each NCAL divided by the maximal cross-sectional vessel area at the proximal reference site. Positive remodeling was defined as an RI > 1.05.

Table 1
Patient characteristics and serum lipid profiles stratified by statin use.

	Statin use			p value
	IS group ($n=24$)	MS group ($n=26$)	NS group ($n=64$)	
Age (yrs)	67.6 ± 7.1	68.4 ± 9.6	67.3 ± 9.6	0.87
Male	17 (71%)	18 (69%)	51 (79%)	0.49
Body mass index (kg/m^2)	24.9 ± 2.6	23.9 ± 3.7	24.2 ± 3.3	0.85
Hypertension	20 (83%)	17 (65%)	39 (61%)	0.14
Diabetes mellitus	12 (50%)	14 (54%)	35 (54%)	0.92
Smoking	16 (64%)	7 (27%)	33 (52%)	0.02
Calcium score	114 (40–623)	143 (46–430)	111 (10–423)	0.92
ACEI/ARB use	14 (52%)	7 (26%)	21 (32%)	0.10
Aspirin use	8 (30%)	15 (56%)	13 (24%)	0.012
Triglycerides (mg/dl)	183.2 ± 99.5	133.0 ± 56.8	164.1 ± 129.1	0.36
LDL-C (mg/dl)	93.3 ± 17.9	115.2 ± 29.6*	124.4 ± 33.5**	<0.001
HDL-C (mg/dl)	57.0 ± 14.5	58.7 ± 19.5	53.8 ± 18.0	0.44
LDL-C/HDL-C	1.74 ± 0.56	2.12 ± 0.76*	2.56 ± 1.04**	<0.001

Data are the number (%), the mean ± SD, or the median (interquartile range). * $p<0.01$, ** $p<0.001$ vs. IS group; IS, intensive statins; MS, moderate statins; NS, no statin; ACEI/ARB, angiotensin-converting enzyme inhibitors or angiotensin II receptor blockers; LDL-C, low-density lipoprotein cholesterol; HDL-C, high-density lipoprotein cholesterol.

2.4. Statistical analysis

Coronary calcium score is expressed as a median value and interquartile range. Other measurements are expressed as mean ± SD. We used the Mann–Whitney test and analysis of variance, including Tukey's test for multiple comparisons, to compare continuous variables between the groups. Categorical variables are reported as number (%) and were compared using Pearson's chi-square test. We used Pearson's correlation coefficient to compare minimum plaque CT density in each patient with serum LDL-C levels.

We calculated odd ratios (OR) with 95% confidence intervals (CI) with adjustment for age, gender, and traditional coronary risk factors including hypertension, diabetes, smoking and drug usage.

All analyses were performed using SPSS16.0 (SPSS Japan Inc, Tokyo, Japan). A p value of <0.05 was considered statistically significant.

3. Results

During contrast-enhanced CT scanning, mean heart rate was 63.0 ± 8.0 beats/min, and mean scan time was 6.4 ± 1.9 s. No patient experienced any complications due to the CT scanning.

Table 1 shows clinical characteristics of the three groups. Cigarette smoking was less frequent in the MS group. ACEI/ARB were more frequently used in the IS group, and aspirin in the MS group. Serum LDL-C levels (93.3 ± 17.9 mg/dl, 115.2 ± 29.6 mg/dl, 124.4 ± 33.5 mg/dl, $p<0.001$) and LDL-C/HDL-C ratio (1.74 ± 0.56, 2.12 ± 0.76, 2.56 ± 1.04, $p<0.001$) were lower in the IS group than the other groups.

A total of 235 NCALs were observed in 114 patients. Table 2 shows the comparison of NCAL findings among the three groups classified by statin use (IS: 50 lesions; MS: 45

Table 2
Lesion-based characteristics and analysis of NCALs stratified by statin use.

Lesions	Statin use			p value
	IS group ($n=50$)	MS group ($n=45$)	NS group ($n=138$)	
Plaque location				
Left anterior descending	20 (40%)	16 (36%)	53 (38%)	
Left circumflex	10 (20%)	4 (9%)	29 (21%)	0.47
Left main trunk	6 (12%)	5 (11%)	15 (11%)	
Right	14 (28%)	20 (44%)	41 (30%)	
Obstructive (≥ 75% stenosis)	8 (16%)	8 (18%)	28 (19%)	0.88
CT density (HU)				
Reference lumen	364.1 ± 37.0	353.3 ± 50.6	347.8 ± 56.5	0.17
Plaque	54.5 ± 25.7	41.2 ± 28.9*	40.5 ± 27.1**	0.007
Low-density plaque (≤ 38 HU)	14 (28%)	22 (49%)	72 (52%)	0.013
RI	1.00 ± 0.19	1.06 ± 0.17*	1.09 ± 0.18**	0.024
Positive remodeling lesion (RI > 1.05)	17 (34%)	23 (51%)	70 (51%)	0.10
Low-density plus positive remodeling	10 (10%)	17 (38%)	57 (41%)	0.026
Spotty calcification	18 (36%)	19 (42%)	47 (34%)	0.61

Data are the number (%) of lesions or the mean ± SD. * $p<0.01$, ** $p<0.001$ vs. IS group; NCAL, non-calcified coronary atherosclerotic lesion; IS, intensive statins; MS, moderate statins; NS, no statin; CT, computed tomography; HU, Hounsfield unit; RI, Remodeling index.

Please cite this article as: Kitagawa T, et al, Effects of statin therapy on non-calcified coronary plaque assessed by 64-slice computed tomography, Int J Cardiol (2010), doi:10.1016/j.ijcard.2010.03.005

Table 3
Patient-based comparison of NCAL characteristics stratified by statin use.

Patients	Statin use			p value
	IS group ($n=24$)	MS group ($n=26$)	NS group ($n=64$)	
Numbers of plaques	2.08 ± 0.93	1.76 ± 1.10	2.16 ± 0.96	0.10
Minimum CT density (HU)	43.9 ± 26.4	37.6 ± 35.2	26.7 ± 23.6*#	0.024
Low-density plaque (≤38 HU)	11 (46%)	15 (58%)	51 (80%)	0.009
Numbers of lipid-rich NCAL	0.58 ± 0.72	0.85 ± 0.92*	1.19 ± 0.89*#	0.007
Maximum RI	1.07 ± 0.21	1.09 ± 0.19	1.18 ± 0.18*	0.036
Positive remodeling NCAL (RI > 1.05)	13 (54%)	15 (58%)	48 (75%)	0.10
Numbers of positive remodeling NCAL	0.67 ± 0.70	0.88 ± 1.14	1.09 ± 0.83	0.052
Low-density plus positive remodeling	10 (42%)	13 (50%)	42 (66%)	0.09
Spotty calcification	14 (58%)	14 (54%)	34 (53%)	0.90

Data are the number (%) or the mean ± SD. *$p<0.05$ vs. IS group, #$p<0.01$ vs. MS group. NCAL, non-calcified coronary atherosclerotic lesion; IS, intensive statins; MS, moderate statins; NS, no statin; CT, computed tomography; HU, Hounsfield unit; RI, Remodeling index.

lesions; and NS: 138 lesions). The location, size, proportion of obstructive lesions, and adjacent spotty calcification of NCALs were similar among the three groups. The IS group had a higher mean NCAL CT density (IS: 54.5 ± 25.7 HU, MS: 41.2 ± 28.9 HU, NS: 40.5 ± 27.1 HU, $p=0.007$) and a lower mean RI (IS: 1.00 ± 0.19, MS: 1.06 ± 0.17, NS: 1.09 ± 0.18, $p=0.024$) than the other groups. There were no differences in density of the reference site lumens between the three groups.

Table 3 shows patient-based comparison of the NCALs. The minimum plaque CT density in each patient was 43.9 ± 26.4 HU, 37.6 ± 35.2 HU, and 26.7 ± 23.6 HU in the IS, MS, and NS groups, respectively ($p=0.024$). Frequency of low-density plaque was 46%, 58%, and 78% in the IS, MS, and NS groups, respectively, ($p=0.009$). The IS group had fewer low-density NCALs than the other groups (IS: 0.58 ± 0.72, MS: 0.85 ± 0.92, NS: 1.19 ± 0.89, $p=0.007$). A higher proportion of the NS group tended to have positive remodeling lesions (IS: 54%, MS: 58%, NS: 75%, $p=0.10$) and patients in the NS group tended to have a greater number of positive remodeling lesions (IS: 0.67 ± 0.70, MS: 0.88 ± 1.14, NS: 1.09 ± 0.83, $p=0.052$).

We also found an inverse correlation between serum LDL-C level and the minimum plaque CT density ($r=-0.28$, $p=0.002$, Fig. 1). According to the regression equation, a CT density of 38 HU corresponded with LDL-C of 100 mg/dl. A higher proportion of patients in the IS group had LDL-C levels <100 mg/dl (IS: 71%, MS: 27%, NS: 20%, $p<0.001$). In addition, multivariate analysis showed that intensive statin use independently reduced the risk of low-density NCALs compared with the other two groups (OR 0.55, 95% CI 0.32–0.91, $p=0.02$).

Table 4 shows serum lipid profiles classified by the number of low-density lesions per patient. Patients with two or more low-density NCALs had higher serum LDL-C levels and lower HDL-C levels than patients with fewer lesions and, thus, a significantly higher LDL-C/HDL-C ratio. The adjusted OR for multiple low-density plaques when LDL-C/HDL-C > 2.5 was 2.39 (95%CI 1.28–4.86, $p<0.001$).

4. Discussion

We used 64-slice CTA to show that low-density NCALs are less common in patients with stable coronary atherosclerosis after >6 months of intensive statin treatment than in patients on moderate or no statin treatment. Intensive statin use was more strongly

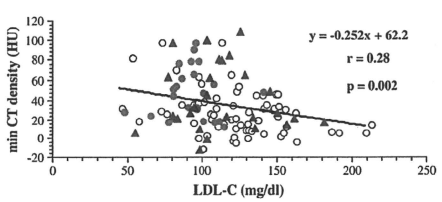

Fig. 1. The lowest plaque CT density in each patient was negatively correlated with serum low-density lipoprotein cholesterol (LDL-C) level. A CT density of 38 Hounsfield unit (HU) corresponded with LDL-C of 100 mg/dl. LDL-C level <100 mg/dl was achieved in 71%, 27%, and 20% of patients treated with intensive statins (red closed circle), moderate statins (blue closed triangle), and no statins (black open circle) respectively.

Table 4
Comparison of serum lipid profiles stratified by the number of lipid-rich NCALs per patient.

Patients	No lesions ($n=35$)	1 lesion ($n=54$)	≥2 lesions ($n=25$)	p value
Age (yrs)	67.9 ± 7.6	67.1 ± 10.0	68.2 ± 9.2	0.88
Male (%)	20 (57%)	46 (85%)	20 (80%)	0.009
Body mass index (kg/m^2)	24.9 ± 3.2	23.9 ± 3.6	24.1 ± 2.4	0.38
Triglyceride (mg/dl)	130.5 ± 66.6	137.1 ± 142.8	167.0 ± 68.1	0.13
LDL-C (mg/dl)	106.1 ± 22.2	114.9 ± 34.7	131.2 ± 33.2*#	0.014
HDL-C (mg/dl)	60.6 ± 17.2	56.6 ± 18.9	46.2 ± 11.4*#	0.006
LDL-C/HDL-C	1.88 ± 0.59	2.24 ± 0.97	2.98 ± 1.00*#	<0.001
Intensive statin use	13 (54%)	8 (33%)	3 (13%)	0.03
Moderate statin use	11 (31%)	10 (18%)	5 (20%)	0.31
No statin use	11 (31%)	36 (67%)	17 (68%)	<0.001

Data are the number (%) or the mean ± SD. *$p<0.01$, vs. none group, #$p<0.05$, ##$p<0.01$ vs. 1 lesion group. NCAL, non-calcified coronary atherosclerotic lesion; LDL-C, low-density lipoprotein cholesterol; HDL-C, high-density lipoprotein cholesterol.

associated with a reduction in lipid-rich plaque components, indicated by fewer low-density plaques, than with a reduction in positive vascular remodeling. Qualitative changes may thus precede quantitative changes in the process of coronary plaque stabilization. Intensive statin use stabilizes coronary plaques by reducing serum LDL-C level <100 mg/dl [17], and we found a close relationship between the LDL-C/HDL-C ratio and the number of low-density plaques. Our results indicate that non-invasive coronary CTA is useful for detecting NCALs and assessing changes in plaque characteristics in patients on lipid-lowering therapy.

4.1. Effect of intensive statin on coronary plaque characteristics

Recent serial analysis with IVUS and angioscopy [7] showed volume reduction and an early loss of yellow color in plaques in patients with stable coronary artery disease receiving atorvastatin. A previous study using 16-slice CT also found that atorvastatin therapy significantly increased plaque density [18]. Improved CTA resolution now allows reliable analysis of plaques comparable with IVUS [12,19].

Previous studies using IVUS have reported that intensive statin therapy reduces serum LDL-C levels, resulting in significant regression of plaque volume, but could not assess changes in plaque composition [3–7]. Our CTA data show that patients with chronic stable coronary disease have significantly lower RI and fewer positive remodeling lesions after six months of intensive statin treatment than those on moderate or no statin treatment.

Our data also show that the combination of low-density plaques and positive remodeling occurs less frequently in patients treated with intensive statin therapy. We have previously reported that these indicators of NCAL vulnerability are closely correlated and may work synergistically in increasing the risk of ACS [12]. Our findings indicate that intensive statin therapy not only reduces the number of lipid-rich coronary plaques but also inhibits characteristic changes in vulnerable coronary plaques.

4.2. Statin effects on LDL-C and HDL-C

In the present study, we found an inverse correlation between serum LDL-C level and the minimum plaque CT density. Our regression equation predicts that 38 HU, the cut-off value we used to define low-density plaque, corresponds to an LDL-C level of 100 mg/dl. A recent report demonstrates that LDL-C level after intensive statin therapy is 70 mg/dl or less [2]. However, our results are consistent with the Japanese guidelines for lipid management that suggest a target level of LDL-C<100 mg/dl [20]. In the present study, patients with LDL-C<100 mg/dl had a 0.55-fold risk ratio of having lipid-rich plaques. We suggest that lipid-lowering therapy using intensive statins may reduce the number of lipid-rich NCALs. As our

Please cite this article as: Kitagawa T, et al, Effects of statin therapy on non-calcified coronary plaque assessed by 64-slice computed tomography, Int J Cardiol (2010), doi:10.1016/j.ijcard.2010.03.005

data shows an inverse correlation between minimum plaque CT density and serum LDL-C level, more aggressive lipid lowering therapy (a target LDL-C level of <70 mg/dl) would be effective to reduce the lipid-rich component (plaque CT density would be higher).

We also found that a higher LDL-C/HDL-C ratio is correlated with larger numbers of low-density plaques on CTA. However, there was no significant relationship between LDL-C/HDL-C and the number of positive remodeling lesions. Nicholls et al. [8] demonstrated that statin therapy is associated with regression of coronary atherosclerosis when LDL-C is substantially reduced and HDL-C increased by more than 7.5%. Moreover, greater numbers of low-density plaques were found in patients with low HDL-C. Amano et al. reported that the metabolic syndrome, for which low HDL-C is one of the diagnostic criteria, was associated with lipid-rich plaques and mild to moderate coronary lesions [21]. Gama et al. found an inverse relationship between HDL-C and coronary events in patients with LDL-C<60 mg/dl, but could not determine whether statin use attenuates the risks associated with low HDL-C [22]. In our data, patients with large numbers of low-density plaques, assumed to be lipid-rich plaques, had higher LDL-C levels and lower HDL-C levels. Lipid-lowering with intensive statin treatment may stabilize NCALs by reducing lipid-rich components in the plaques and the increase in HDL-C levels may help to decrease the number of low-density plaques.

4.3. Study limitations

This is a cross-sectional study and we did not evaluate changes in serum lipid profile during statin therapy. However, we have demonstrated that over six months of statin treatment is effective to stabilize vulnerable coronary plaques [3].

We found some differences in baseline patient characteristics in our data with respect to cigarette smoking and medication use. ACEI/ARBs were more frequently used in the IS group. As ACEI/ARBs have an independent effect on plaque stability, this may have affected our results.

Although the IS group included three different statins, atorvastatin, rosuvastatin, and pitavastatin, previous studies have reported these statins to have similar effects on lipid levels and plaque stability [2–5]. Non-culprit lesions in ACS patients showed similar reductions in plaque volume and serum LDL-C level in patients treated with atorvastatin and pitavastatin [5].

The present study is also limited by the lack of measurement of inflammatory markers such as C-reactive protein (CRP) [23]. In our preliminary data, CRP levels were significantly higher in the NS group than the statin groups, but not between the IS and MS groups. Higher frequency of aspirin use in the MS group may have reduced any difference in CRP levels between the IS and MS groups. Ongoing prospective trials, including the plaque registration and evaluation detected in CT (PREDICT) study (ClinicalTrials.gov ID: NCT00991835) will monitor the effect of improving serum lipid profiles on coronary plaque stabilization, particularly with respect to the LDL-C/HDL-C ratio and serum CRP levels [23,24].

5. Conclusions

Our CTA findings indicate that lipid-lowering therapy, particularly intensive statin treatment, stabilizes coronary plaques. Cardiac CTA may prove a useful non-invasive modality for assessing the effects of lipid-lowering therapy on NCAL characteristics in patients with coronary artery disease.

Acknowledgment

The authors of this manuscript have certified that they comply with the Principles of Ethical Publishing in the International Journal of Cardiology [25].

References

[1] Scandinavian Simvastatin Survival Study Group. Randomized trial of cholesterol lowering in 4,444 patients with coronary artery disease. Lancet 1994;344:1383–8.
[2] Ridker PM, Danielson E, Fonseca FA, et al. Rosuvastatin to prevent vascular events in men and women with elevated C-reactive protein. N Engl J Med 2008;359: 2195–207.
[3] Okazaki S, Yokoyama T, Miyauchi K, et al. Early statin treatment in patients with acute coronary syndrome: demonstration of the beneficial effect on atherosclerotic lesions by serial volumetric intravascular ultrasound analysis during half a year after coronary event: the ESTABLISH Study. Circulation 2004;110:1061–8.
[4] Nissen SE, Tuzcu EM, Schoenhagen P, et al. Effect of intensive compared with moderate lipid-lowering therapy on progression of coronary atherosclerosis: a randomized trial. JAMA 2004;291:1071–80.
[5] Hiro T, Kimura T, Morimoto T, et al. Effect of intensive statin therapy on regression of coronary atherosclerosis in patients with acute coronary syndrome: a multicenter randomized trial evaluated by volumetric intravascular ultrasound using pitavastatin versus atorvastatin (JAPAN-ACS (Japan assessment of pitavastatin and atorvastatin in acute coronary syndrome) study). J Am Coll Cardiol 2009;54:293–302.
[6] Schoenhagen P, Tuzcu EM, Apperson-Hansen C, et al. Determinants of arterial wall remodeling during lipid-lowering therapy: serial intravascular ultrasound observations from the reversal of atherosclerosis with aggressive lipid-lowering therapy (REVERSAL) trial. Circulation 2006;113:2826–34.
[7] Hirayama A, Saito S, Ueda Y, et al. Qualitative and quantitative changes in coronary plaque associated with atorvastatin therapy. Circ J 2009;73:718–25.
[8] Nicholls SJ, Tuzcu EM, Sipahi I, et al. Statins, high-density lipoprotein cholesterol, and regression of coronary atherosclerosis. JAMA 2007;297:499–508.
[9] Schroeder S, Kopp AF, Baumbach A, et al. Noninvasive detection and evaluation of atherosclerotic coronary plaques with multislice computed tomography. J Am Coll Cardiol 2001;37:430–5.
[10] Funabashi N, Asano M, Komuro I. Predictors of non-calcified plaques in the coronary arteries of 242 subjects using multislice computed tomography and logistic regression models. Int J Cardiol 2007;117:191–7.
[11] Motoyama S, Kondo T, Sarai M, et al. Multislice computed tomographic characteristics of coronary lesions in acute coronary syndromes. J Am Coll Cardiol 2007;50:319–26.
[12] Kitagawa T, Yamamoto H, Ohhashi N, et al. Comprehensive evaluation of non-calcified coronary plaque characteristics detected using 64-slice computed tomography in patients with proven or suspected coronary artery disease. Am Heart J 2007;154:1191–8.
[13] Kitagawa T, Yamamoto H, Horiguchi J, et al. Characterization of noncalcified coronary plaques and identification of culprit lesions in patients with acute coronary syndrome by 64-slice computed tomography. JACC Cardiovasc Imaging 2009;2:153–60.
[14] Braunwald E, Antman EM, Beasley JW, et al. ACC/AHA 2002 guideline update for the management of patients with unstable angina and non-ST-segment elevation myocardial infarction-summary article: a report of the American College of Cardiology/American Heart Association task force on practice guidelines (Committee on the Management of Patients With Unstable Angina). Circulation 2002;106:1893–900.
[15] Agatston AS, Janowitz WR, Hildner FJ, et al. Quantification of coronary artery calcium using ultrafast computed tomography. J Am Coll Cardiol 1990;15:827–32.
[16] Ohashi N, Yamamoto H, Horiguchi J, et al. Visceral fat accumulation as a predictor of coronary artery calcium as assessed by multislice computed tomography in Japanese patients. Atherosclerosis 2009;202:192–9.
[17] Brunzell JD, Howard BV, Davidson M, et al. Lipoprotein management in patients with cardiovascular risk; consensus conference report from the American Diabetes Association and the American College of Cardiology Foundation. J Am Coll Cardiol 2008;51:1512–24.
[18] Uehara M, Funabashi N, Mikami Y, et al. Quantitative effect of atorvastatin on size and content of non-calcified plaques of coronary arteries 1 year after atorvastatin treatment by multislice computed tomography. Int J Cardiol 2008;130:269–75.
[19] Achenbach S, Moselewski F, Ropers D, et al. Detection of calcified and noncalcified coronary atherosclerotic plaque by contrast-enhanced, submillimeter multidetector spiral computed tomography: a segment-based comparison with intravascular ultrasound. Circulation 2004;109:14–7.
[20] Teramoto T, Sasaki J, Ueshima H, et al. Risk factors of atherosclerotic diseases. Executive summary of Japan Atherosclerosis Society (JAS) guideline for diagnosis and prevention of atherosclerosis cardiovascular disease for Japanese. J Atheroscler Thromb 2007;14:267–77.
[21] Amano T, Matsubara T, Uetani T, et al. Impact of metabolic syndrome on tissue characteristics of angiographically mild to moderate coronary lesions: integrated backscatter intravascular ultrasound study. J Am Coll Cardiol 2007;49:1149–56.
[22] deGoma EM, Leeper NJ, Heidenreich PA. Clinical significance of high-density lipoprotein cholesterol in patients with low low-density lipoprotein cholesterol. J Am Coll Cardiol 2008;51:49–55.
[23] Ridker PM, Rifai N, Lowenthal SP, et al. Measurement of C-reactive protein for the targeting of statin therapy in the primary prevention of acute coronary events. N Eng J Med 2001;344:1959–65.
[24] Tang TY, Howarth SP, Miller SR, et al. The ATHEROMA (atorvastatin therapy: effects on reduction of macrophage activity] study: evaluation using ultrasmall superparamagnetic iron oxide-enhanced magnetic resonance imaging in carotid disease. J Am Coll Cardiol 2009;53:2039–50.
[25] Coats AJ. Ethical authorship and publishing. Int J Cardiol 2009;131:149–50.

Please cite this article as: Kitagawa T, et al, Effects of statin therapy on non-calcified coronary plaque assessed by 64-slice computed tomography, Int J Cardiol (2010), doi:10.1016/j.ijcard.2010.03.005

Circulation Journal
Official Journal of the Japanese Circulation Society
http://www.j-circ.or.jp

Evaluation of Severely Calcified Coronary Artery Using Fast-Switching Dual-kVp 64-Slice Computed Tomography

Minoru Yamada; Masahiro Jinzaki, MD; Yasuhiro Imai; Shun Yamazaki, MD; Nobuaki Imanishi, MD; Yutaka Tanami, MD; Akihisa Yamazaki; Sadakazu Aiso, MD; Sachio Kuribayashi, MD

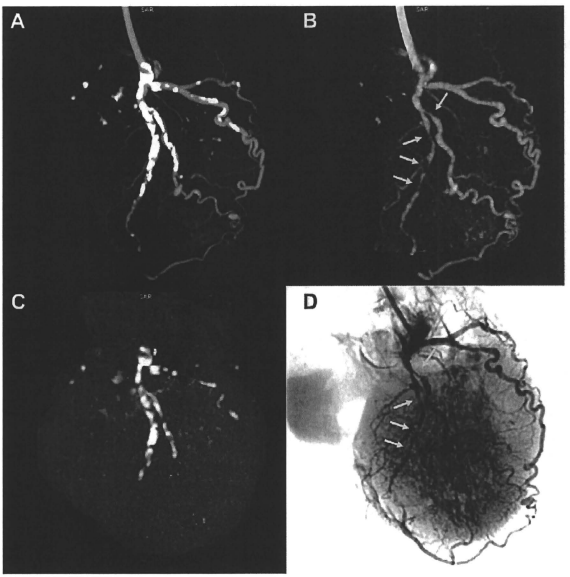

Figure. (**A**) Maximum-intensity projection (MIP) image generated by single-kVpeak (kVp) computed tomography (CT). (**B**) MIP iodine-density image generated by fast-switching dual-kVp CT. (**C**) MIP calcium-density image generated by fast-switching dual-kVp CT. (**D**) Conventional coronary angiography (CAG). The significant stenotic regions in the left anterior descending artery and diagonal branch (**B**, arrows) are clearly demonstrated in the MIP iodine-density image generated by fast-switching dual-kVp CT, which corresponded well to the CAG findings (**D**, arrows). These findings could not be evaluated on the MIP images generated by single-kVp CT (**A**) due to severe calcification.

Received July 2, 2010; revised manuscript received September 10, 2010; accepted October 5, 2010; released online December 2, 2010
Time for primary review: 25 days

Multi-dimension Biomedical Imaging & Information Laboratory in Research Park (M.Y.), Department of Diagnostic Radiology (M.J., Y.T., A.Y., S.K.) and Clinical Anatomy Laboratory (S.Y., N.I., S.A.), Keio University School of Medicine, Tokyo; and CT Engineering, GE Healthcare Japan, Tokyo (Y.I.), Japan
Mailing address: Masahiro Jinzaki, MD, Department of Diagnostic Radiology, Keio University School of Medicine, 35 Shinanomachi, Shinjuku-ku, Tokyo 160-8582, Japan. E-mail: jinzaki@sc.itc.keio.ac.jp

ISSN-1346-9843 doi:10.1253/circj.CJ-10-0636

The introduction of 64-slice computed tomography (CT) has enabled non-invasive evaluation of coronary artery stenosis with a high degree of accuracy. A large number of studies, however, have found that the presence of severely calcified plaques is the most frequent reason for false-positive or false-negative evaluation, limiting the clinical usefulness of 64-slice CT.[1–8] Dual-kVpeak (kVp) CT allows material decomposition between calcification and iodine.[9] CT system parameters, however, for instance gantry rotation speed, data sampling speed, and X-ray tube power output, have not been sufficient for routine clinical use.

Recently, fast-switching dual-kVp technology, dynamic switching between 80- and 140-kVp X-rays in <0.5 ms, which uses simultaneous dataset acquisition at both energies in one gantry rotation, has been developed. Because of the extremely small time difference, the acquisition datasets at 80 and 140 kVp are treated as coincident projection data both temporally and spatially. Use of this fast-switching dual-kVp technology has recently been enabled in 64-slice CT by the development of a garnet crystal scintillation detector with ultra-fast optical response, and of a high-voltage generator with ultra-fast tube voltage switching. In addition, the data acquisition system of that CT allows data sampling at more than 2.5-fold in one gantry rotation compared with a conventional 64-slice CT, hence, data acquisition that maintains in-plane spatial resolution and flux balance between 80 and 140 kVp is achieved. The fast-switching dual-kVp data acquisition enables attenuation measurements to be mathematically transformed into density (or amount) for 2 basis materials in projection data space. This projection-based process corrects for multi-material beam hardening effects, which provides accurate material decomposition in material density units. Generally, water and iodine are selected as the basis material pair. The respective pair of desired material density images (iodine and calcium) can be generated by transformation of these 2 basis material density images in the material decomposition process.[10] Because this technology has not yet been applicable to clinical cardiac scanning, we applied this technology to ex vivo human heart specimens.

An ex vivo human heart specimen was taken from the clinical anatomy laboratory of Keio University after institutional review board approval. The specimen, after being put into a chest phantom (Kyoto-kagaku, Japan), was scanned using high-definition CT (HDCT; Discovery CT750 HD, GE Healthcare, WI, USA) in both the single-kVp (120 kVp) and fast-switching dual-kVp (80 and 140 kVp) helical scanning modes, immediately after injection of a mixture of iodinated contrast medium (Iohexol; Daiichi-sankyo, Japan) and polyethylene glycol (CT value: 350 HU at 120 kVp) into the ostium of the left coronary artery. The radiation dose estimated for the fast-switching dual-kVp helical scanning mode was 14 mSv, which is within the range used in conventional coronary CT angiography (8–18 mSv).[11] Conventional coronary angiography (CAG) was also performed using a flat-panel digital detector system (Innova 3100, GE Healthcare) as the reference standard for the coronary artery stenosis findings.

In the single-kVp CT image it was difficult to evaluate the degree of stenosis in the left anterior descending artery, diagonal branch or left circumflex artery, where severely calcified plaques existed (**Figure A**). Iodine-density and calcium-density images were generated from fast-switching dual-kVp CT data (**Figures B, C**). The significant stenotic regions were clearly demonstrated in the iodine-density image (**Figure B**, arrows), which corresponded well to the CAG findings (**Figure D**, arrows).

Although the present study was limited by not having been conducted on a beating heart, we conclude that fast-switching dual-kVp technology may be useful for the evaluation of severely calcified coronary arteries and may overcome the limitations of conventional CT.

References

1. Abdulla J, Abildstrom SZ, Gotzsche O, Christensen E, Kober L, Torp-Pedersen C. 64-multislice detector computed tomography coronary angiography as a potential alternative to conventional coronary angiography: A systematic review and meta-analysis. *Eur Heart J* 2007; **28:** 3042–3050.
2. Ropers D, Baum U, Pohle K, Anders K, Ulzheimer S, Ohnesorge B, et al. Detection of coronary artery stenoses with thin-slice multi-detector row spiral computed tomography and multiplanar reconstruction. *Circulation* 2003; **107:** 664–666.
3. Raff GL, Gallagher MJ, O'Neill WW, Goldstein JA. Diagnostic accuracy of noninvasive coronary angiography using 64-slice spiral computed tomography. *J Am Coll Cardiol* 2005; **46:** 552–557.
4. Mollet NR, Cademartiri F, van Mieghem CA, Runza G, McFadden EP, Baks T, et al. High-resolution spiral computed tomography coronary angiography in patients referred for diagnostic conventional coronary angiography. *Circulation* 2005; **112:** 2318–2323.
5. Goldstein JA, Gallagher MJ, O'Neill WW, Ross MA, O'Neil BJ, Raff GL. A randomized controlled trial of multi-slice coronary computed tomography for evaluation of acute chest pain. *J Am Coll Cardiol* 2007; **49:** 863–871.
6. Jinzaki M, Sato K, Tanami Y, Yamada M, Anzai T, Kawamura A, et al. Diagnostic accuracy of angiographic view image for the detection of coronary artery stenoses by 64-detector row CT. *Circ J* 2009; **73:** 691–698.
7. Ueno K, Anzai T, Jinzaki M, Yamada M, Jo Y, Maekawa Y, et al. Increased epicardial fat volume quantified by 64-multidetector computed tomography is associated with coronary atherosclerosis and totally occlusive lesions. *Circ J* 2009; **73:** 1927–1933.
8. Matsumoto N, Nagao K, Hirayama A, Sato Y. Non-invasive assessment and clinical strategy of stable coronary artery disease by magnetic resonance imaging, multislice computed tomography and myocardial perfusion SPECT. *Circ J* 2010; **74:** 34–40.
9. Kalender WA, Perman WH, Vetter JR, Klotz E. Evaluation of a prototype dual-energy computed tomographic apparatus. I: Phantom studies. *Med Phys* 1986; **13:** 334–339.
10. Wu X, Langan DA, Xu D, Benson TM, Pack JD, Schmitz AM, et al. Monochromatic CT image representation via fast switching dual kVp. *Proc SPIE* 2009; **7258:** 725845.
11. Hausleiter J, Meyer T, Hermann F, Hadamitzky M, Krebs M, Gerber TC, et al. Estimated radiation dose associated with cardiac CT angiography. *JAMA* 2009; **301:** 500–507.

Int J Cardiovasc Imaging
DOI 10.1007/s10554-010-9786-x

ORIGINAL PAPER

Improvement of in-stent lumen measurement accuracy with new High-Definition CT in a phantom model: comparison with conventional 64-detector row CT

Yutaka Tanami · Masahiro Jinzaki · Minoru Yamada · Yasuhiro Imai · Koji Segawa · Sachio Kuribayashi

Received: 30 September 2010 / Accepted: 23 December 2010

Abstract The purpose of this study was to evaluate improvement of measurement accuracy of in-stent lumen using coronary stent phantoms on new High-Definition CT (HDCT) compared with conventional 64 detector-row CT (MDCT). To estimate the spatial resolution, a high-resolution insert of CATPHAN (The Phantom Laboratory, NY, USA) was scanned by both HDCT (Discovery CT750 HD) and MDCT (LightSpeed VCT). Also, we developed six types of stent phantom, which have 2.5- and 3.0-mm-diameter with three different types of stents (Velocity: Johnson & Johnson, Driver: Medtronic, Multilink-Rx: Guidant). A 50% stenotic segment made of acrylic resin was built at the center inside the stent. Those coronary vessel phantoms were made of acrylic resin and filled with diluted Iodine (350 HU in 120 kVp), and each stent was fixed inside of those vessels. Those phantoms in water-filled tank were scanned on both HDCT and MDCT. The luminal diameter obtained using digital calipers at five different points and the mean luminal diameter (MLD) were calculated. The underestimate ratio (UR) and △UR was defined as follows: UR = [True diameter of stent—MLD]/True diameter of stent; △UR = [MLD at HDCT—MLD at MDCT]/True diameter of stent. The spatial resolution was estimated to be 0.71 mm on MDCT and 0.50 mm on HDCT. At the non-stenotic segments, the △URs were 11.6% (Velocity), 16.4% (Driver) and 7.2% (Multilink) for the 2.5-mm stents, and 14.0% (Velocity), 16.3% (Driver) and 13.3% (Multilink) for the 3.0-mm stents. At the stenotic segment, the △URs were 23.2% (Velocity), 8.0% (Driver) and 13.6% (Multilink) for the 2.5-mm stents, and 20.0% (Velocity), 14.7% (Driver) and 15.3% (Multilink) for the 3.0-mm stents. Superior spatial resolution of HDCT could be promising for more accurate measurement of in-stent diameter.

Keywords in-stent restenosis · Computed tomography · Coronary artery

Y. Tanami · M. Jinzaki (✉) · S. Kuribayashi
Department of Radiology, Keio University School of Medicine, 35 Shinanomachi, Shinzyuku-ku, Tokyo 160-8582, Japan
e-mail: jinzaki@rad.med.keio.ac.jp

M. Yamada
Research Park, School of Medicine, Keio University, 35 Shinanomachi, Shinjuku-ku, Tokyo 160-8582, Japan

Y. Imai
CT Engineering, GE Healthcare Japan, 4-7-127 Asahigaoka, Hino-Shi, Tokyo 191-8503, Japan

K. Segawa
CT Customer Application, GE Healthcare Japan, 4-7-127 Asahigaoka, Hino-Shi, Tokyo 191-8503, Japan

Published online: 08 January 2011

Introduction

Coronary artery disease (CAD) is one of the leading causes of death. In recent years, coronary artery stent placement has been used as a routine procedure to